

Anti-Correlation Digital Halftoning by Generalized Russian Roulette

Dmitri A. Gusev
Computer Science Department
Indiana University
Lindley Hall, Rm 215
Bloomington, IN 47405

Abstract

A new class of digital halftoning algorithms is introduced. Anti-correlation digital halftoning (ACDH) combines the idea of a well-known game, Russian roulette, with the statistical approach to bilevel quantization of images. A representative of the class, serpentine anti-correlation digital halftoning, is described and compared to error diffusion, ordered dither, and other important digital halftoning algorithms. Digital halftoning means image quantization by algorithms that exploit properties of the vision system to create the illusion of continuous tone. Common problems often accompanying digital halftoning include contouring, correlated artifacts, edge enhancement, and unpleasant boundary effects. Serpentine ACDH causes fewer unwanted correlated artifacts and less contouring than the benchmark algorithms. Two intensity distortion criteria similar to those applied earlier to evaluate quality of non-uniform sampling are used to demonstrate that serpentine ACDH represents the average intensity remarkably well. Unlike popular algorithms based on error diffusion, serpentine ACDH does not enhance edges. A simple preprocessing technique allows one to introduce edge enhancement if desired, while keeping it more isotropic than that of error diffusion. Serpentine ACDH does not cause significant boundary effects.

1. Introduction

Inherent limitations of devices for image visualization and printing often require quantization of two-dimensional digital images to a limited number of grayscale levels. The case of bilevel quantization is of particular interest when an image is to be printed on a printer that can only produce black-and-white pictures. *Digital halftoning* [31] means image quantization by algorithms that exploit properties of the vision system to create the illusion of continuous tone. Digital halftoning algorithms have been applied in digital holography [28], medical imaging [25], pattern recognition [16], and many other areas (see references in [15]).

We will be dealing with rectangular input and output digital images consisting of pixels on a common square grid. Other cases are considered elsewhere [30, 31, 34]. Let the input of a digital halftoning algorithm be a two-dimensional digital grayscale image G represented by an $N_1 \times N_2$ matrix of real values $g_{i,j} \in [0, 1]$. In bilevel quantization, a binary image B represented by an $N_1 \times N_2$ matrix of $b_{i,j} \in \{0, 1\}$ serves as output of the algorithm. The symbols $g_{i,j}$ and $b_{i,j}$ stand for *intensities* of pixels on the grid, where $i = 0, 1, \dots, N_1 - 1$ and $j = 0, 1, \dots, N_2 - 1$ respectively indicate line and column of a pixel. An intensity value 0 means “black”, 1 means “white”. To determine how G should be reproduced, proper meanings must be assigned to the intensity values in $(0, 1)$. This task can be accomplished as described in [15]. Bayer [4] popularized a class of digital halftoning algorithms called *ordered dither*. Figures 1 (a) and 2 (a) feature two test image representations obtained by ordered dither with an 8×8 *dither matrix* from [19]. Such dither matrices can be produced by the method of *recursive tessellation* [32]. The images are printed at the resolution of 300 dots per inch (dpi). Among the modifications of ordered dither, a prominent place belongs to Ulichney’s *void-and-cluster* method [33] involving special dither matrices called *blue noise masks* [22]. The method is based on the concept of *blue noise* [31]. Images in Figures 1 (b) and 2 (b) were obtained by ordered dither with a 128×128 blue noise mask generated using the void-and-cluster method. The method’s internal parameter $\sigma = 1.5$. *Error diffusion (ED)* [12] is another important class of digital halftoning algorithms. The error diffusion algorithms employ matrices of *weights*, or *error diffusion coefficients*, and are sometimes classified by the number of non-zero weights. Ulichney [31] studied *error diffusion on a serpentine raster*, aka *serpentine error diffusion (SED)*. Sandler et al. [25] explained the advantage of SED and described a relatively fast three-weight version of SED. This version was used to produce the images shown in Figures 1 (c) and 2 (c). A number of slower algorithms based on ED achieve comparable or lower image quality, see [15]. *Hybrid algorithms* for dig-

ital halftoning have been studied by many researchers, including Knuth [19], Eschbach [9], and Sandler et al. [25]. Eschbach [9] combined error diffusion with another digital halftoning technique, *pulse-density modulation (PDM)*, first proposed in [10]. Halftone images produced by the resulting hybrid algorithm can be seen in Figures 1 (d) and 2 (d). The areas where $1/4 < g_{i,j} < 3/4$ were treated by the classical Floyd–Steinberg ED algorithm [13], and the rest of the image was subjected to PDM. Eschbach recommended use of ED to process regions touching the areas with $1/4 < g_{i,j} < 3/4$ as well, in order to break up the seams seen at the switching points. However, this causes highly visible patches to emerge in very light and very dark areas adjoining such points. Several so-called *iterative algorithms* for digital halftoning were studied, including those based on *iterative convolution* [35, 36]. Figures 1 (e) and 2 (e) represent test images halftoned by the iterative convolution algorithm from [35] (30 iterations; internal parameters $\Delta = 0.29$, $\delta = 0.005$, and $a = 0.4$). Other digital halftoning algorithms employ such techniques as patterning [24] (it is also known as pulse-surface-area modulation, or PSAM [31]), hill climbing and simulated annealing [2, 7], look-up-table based halftoning [21], etc. (See [15] for a more comprehensive review.)

Following a brief discussion of the halftone image quality issues, I will introduce a new class of digital halftoning algorithms in Section 2.

2. Anti-Correlation Digital Halftoning

In halftone images, artificial contours may sometimes appear in the areas with slowly varying [31] or constant [27] input intensity. This effect is called *contouring* [31]. *Correlated artifacts* [31] present another problem, common for the algorithms that do not generate regular periodic patterns. On the other hand, presence of highly visible regular periodic patterns usually means poor rendition of small details of the image. By *average intensity* of an area of a digital image we mean the ratio of the sum of pixel intensities for this area and the overall number of pixels in it. In digital halftoning, *edge enhancement (EE)* is characterized by the average intensity being below the input intensity on the dark side of the edge and above it on the light side of the edge. We will discuss EE in more detail in Section 3. Error diffusion is often accompanied by unpleasant *transient boundary effects*.

No single technique of image quality evaluation has gained universal acceptance [8]. A review of the techniques can be found in [15]. Sandler et al. [25] proposed to interpret outputs $b_{i,j}$ of a digital halftoning algorithm as values of random variables $\xi_{i,j}$. (Ulichney [31] did it earlier for the case of constant level input.) Using this interpretation, Sandler et al. developed the following *local*

quasi-optimality criterion. Let S be an area of the image, consisting of pixels that are close together (no exact measure of “closeness” specified), and let $T(S)$ be the set of all possible two-element subsets $\{(i_1, j_1), (i_2, j_2)\}$ of S . Let the covariance of ξ_{i_1, j_1} and ξ_{i_2, j_2} be denoted by $\text{cov}(\xi_{i_1, j_1}, \xi_{i_2, j_2})$. Sandler et al. postulated that it is desirable to construct $\xi_{i,j}$ so that the variance

$$V\left(\sum_S \xi_{i,j}\right) = \sum_S V(\xi_{i,j}) + 2 \sum_{T(S)} \text{cov}(\xi_{i_1, j_1}, \xi_{i_2, j_2})$$

is minimum on the condition that the expected values $E(\xi_{i,j}) = g_{i,j}$ for all (i, j) in S . The authors of the criterion pointed out that the underlying assumption that the vision system averages intensity levels of pixels in S with equal weights is just an approximation. They suggested that, “the closer together any two pixels are, the less correlated the corresponding random variables should be (on the condition that their expected values coincide with the inputs).” Radial anisotropy of the vision system measured by Campbell et al. [6] can be accounted for by picking a measure of closeness based on non-Euclidean distance. For any given pair of pixels, significance of correlation between the random variables depends on the viewing conditions. The approach of Sandler et al. fits the results of psychovisual experiments conducted by Burgess et al. [5] and Myers et al. [23]. According to these results, the human observer is strongly influenced by correlated noise, and the detection performance for even a simple task is degraded substantially in its presence.

Russian roulette is a well-known game consisting of spinning the cylinder of a revolver loaded with one cartridge, pointing the muzzle at one’s own head, and pulling the trigger. An early version of Russian roulette was described by Lermontov [20] in 1839. Due to unavailability of actual revolvers, the number of cylinder chambers n was 1, but the probability \wp that a shot is fired successfully if a cartridge is aligned with the barrel when the trigger is pulled was below 1. In our model, \wp is taken to be 1, and the number of loaded cartridges \tilde{g} is allowed to range between 0 and n . The case of multiple players is considered. We assign numbers $0, 1, \dots, n-1$ to the chambers of each revolver cylinder counterclockwise (looking at the muzzle). Consider white-blooded players on an $N_1 \times N_2$ square grid superimposed over a rectangular part of a geometric plane covered with black snow. Whenever a shot is fired, the corresponding player’s blood produces a white pixel. Let $C_{i,j}$ indicate the revolver cylinder of a player at the position (i, j) , and let

$$C_{i,j}[k] = \begin{cases} 1 & \text{if the } k^{\text{th}} \text{ chamber of } C_{i,j} \text{ contains} \\ & \text{a cartridge,} \\ 0 & \text{otherwise,} \end{cases}$$

for $k = 0, 1, \dots, n-1$.

Anti-correlation digital halftoning (ACDH) is a new class of digital halftoning algorithms. It is based on generalized Russian roulette, and multiple “gaps” consisting of empty chambers are allowed in the revolver cylinders. (Error diffusion can be simulated by a version of generalized Russian roulette such that at most one gap is allowed to remain in each loaded revolver cylinder, see my technical report [15] for the details.) The control over correlation between the random variables forming the unordered pairs $\{\xi_{i,j}, \xi_{i-(\ell-1)+\tau_1, j-(\ell-1)+\tau_2}\}$ is achieved by using input-dependent *anti-correlation filters* $K = (k_{\tau_1, \tau_2})$. Other techniques incorporated in ACDH are *boundary randomization (BR)* and the *average intensity control (AIC)*. The AIC mechanism helps to keep the average intensity of the part of the halftone image already computed closer to the average intensity of the corresponding part of the input image. This is achieved by using the *global histogram of the cartridge distribution* \mathcal{H} , an array of

$$\mathcal{H}_k = \sum_{i,j} C_{i,j}[k],$$

$k = 0, 1, \dots, n-1$. *Local weighted histograms of the cartridge distribution* $H(i, j)$ are arrays of

$$H_k(i, j) = \sum_{\substack{\tau_1 \geq 0, \\ \tau_2 \geq 0}} k_{\tau_1, \tau_2} C_{i-(\ell_K-1)+\tau_1, j-(\ell_K-1)+\tau_2}[k],$$

where $\ell_K > 0$ is a constant integer associated with the local anti-correlation filter K . Let $\mathcal{S}(H(i, j))$ be a permutation of $\{0, 1, \dots, n-1\}$ such that

$$\begin{aligned} H_{\mathcal{S}_0(H(i,j))}(i, j) &\leq H_{\mathcal{S}_1(H(i,j))}(i, j) \leq \dots \\ &\leq H_{\mathcal{S}_{n-1}(H(i,j))}(i, j), \end{aligned}$$

and

$$\mathcal{H}_{\mathcal{S}_x(H(i,j))}(i, j) \leq \mathcal{H}_{\mathcal{S}_y(H(i,j))}(i, j)$$

whenever $x < y$ and $H_{\mathcal{S}_x(H(i,j))} = H_{\mathcal{S}_y(H(i,j))}$. If more than one permutation satisfies these conditions, $\mathcal{S}(H(i, j))$ is selected among the eligible permutations at random. The second of the conditions above is responsible for the AIC. Let $\tilde{\mathcal{S}}(H(i, j), \tilde{g}_{i,j})$, an equivalent of $\mathcal{S}(H(i, j))$ with respect to $\tilde{g}_{i,j}$, be defined as a permutation of $\mathcal{S}(H(i, j))$ such that the elements of $\{\mathcal{S}_0(H(i, j)), \mathcal{S}_1(H(i, j)), \dots, \mathcal{S}_{\tilde{g}_{i,j}-1}(H(i, j))\}$ and $\{\mathcal{S}_{\tilde{g}_{i,j}}(H(i, j)), \mathcal{S}_{\tilde{g}_{i,j}+1}(H(i, j)), \dots, \mathcal{S}_{n-1}(H(i, j))\}$ are permuted independently. $\tilde{\mathcal{S}}(H(i, j), \tilde{g}_{i,j})$ can often be computed faster than $\mathcal{S}(H(i, j))$. Let $C^{(m)}$ be the *configuration* (state of the revolver cylinders) after the m^{th} iteration, and let $C^{(0)}$ be some starting configuration. Each iteration involves processing all pixels in some order, which may depend on m and G .

Let $\text{rand}(n_1..n_2)$ denote a function returning a random integer uniformly distributed on $\{n_1, n_1+1, \dots, n_2\}$,

where $n_1 \leq n_2$, and let $\text{int}(x)$ be a function that takes a real number x , and returns an integer obtained by some rounding operation. *Sequential iterative anti-correlation digital halftoning (SIACDH)* is a subclass of ACDH defined algorithmically as follows.

```

r ← rand(0..n-1); m ← 1; set C(0); initialize H;
while the last iteration is not over
  { /* Process all pixels! */
    for i' from 0 to N1N2 - 1 do
      {
        compute pixel coordinates (i, j) depending
        on i', m, and G;
        g̃i,j ← int(gi,jn);
        select K (it may depend on i, j, m, and G);
        compute H(i, j);
        /* BR: All Ci,j[k] outside
        the image are random */
        compute S̃(H(i, j), g̃i,j);
        /* change the state of Ci,j: */
        for k from 0 to n - 1 do
          {
            k' ← S̃k(H(i, j), g̃i,j);
            if k < g̃i,j then Ci,j[k'] ← 1;
              else Ci,j[k'] ← 0;
            update Hk';
          }
        }
      m ← m + 1; /* current Ci,j for all
      (i, j) form C(m) */
    }
  /* Pull the triggers: */
  for i from 0 to N1 - 1 do
    for j from 0 to N2 - 1 do
      bi,j ← Ci,j[r];

```

The outputs $b_{i,j}$ can be interpreted as values of the corresponding random variables $\xi_{i,j}$ with the expected values $E(\xi_{i,j}) = \frac{\tilde{g}_{i,j}}{n} \approx g_{i,j}$.

Serpentine anti-correlation digital halftoning (SACDH) processes pixels on a serpentine raster, using wedge-shaped input-dependent anti-correlation filters. The starting configuration $C^{(0)}$ corresponds to all revolver cylinders being empty. SACDH is a representative of SIACDH, but only one iteration is performed. In my versions of SACDH ($n = 255$ and $n = 192$ were tried), BR is performed by taking the values $C_{i,j}[k]$ for (i, j) outside the image to be

$$C_{i,j}[k] = \begin{cases} 1 & \text{if } \mathbf{r}_{BR} < n\Delta, \\ 0 & \text{otherwise,} \end{cases}$$

where $\Delta = |\tilde{g}_{i,j} - n/2|/n$, and \mathbf{r}_{BR} is a value of a random variable uniformly distributed on $\{0, 1, \dots, \lceil n/2 \rceil\}$ and computed independently whenever an attempt is made to look up the value of $C_{i,j}[k]$ for (i, j) outside the image.

Filter selection for my versions of SACDH is described in Appendix A of [15]. The asymmetry of the filters compensates for the asymmetry of sequential processing. (*Parallel iterative ACDH* is also described in [15].) Figures 1 (f) and 2 (f) show halftone images produced by SACDH ($n = 255$). When examined visually, the gray scale ramps for $n = 192$ did not differ significantly from those for $n = 255$. When the pixel at the position (i, j) is being processed by SACDH, the values of the coefficients k_{τ_1, τ_2} of the local anti-correlation filter K signify how strongly we want $\xi_{i,j}$ and $\xi_{i-(\ell_K-1)+\tau_1, j-(1-2(i \bmod 2))((\ell_K-1)-\tau_2)}$ to be anti-correlated. While strict conditions have to be imposed on error diffusion coefficients to ensure numerical stability [3], making sure that the computation of the histogram entries never causes an overflow is enough to achieve stability when designing anti-correlation filters. As a result, it is relatively simple to break up any unwanted regular binary pattern or correlated artifact by adjusting K . Alas, other unwanted textures often emerge instead, so I had to perform multiple “trial-and-error” cycles similar to those described in [1]. I tried to eliminate all periodic patterns that either seemed obnoxious by themselves, or caused contouring at 72 dpi, 100 dpi, or 300 dpi. In particular, my versions of SACDH suppress contouring, “worms” and fishbone-like artifacts near $g_{i,j} = 1/2$ at the cost of increased granularity in that area, which is located away from the middle of the gray scale ramps due to the *tone scale adjustment* [31]. The less visible diagonal correlated artifacts are favored over those oriented vertically or horizontally. Very light and very dark areas look nice.

3. Average Intensity Representation, Boundary Effects, and Edge Enhancement

To study how well average intensities are preserved by different digital halftoning algorithms, I computed global *intensity distortion* $M = \sum_{i=0}^{N-1} \sum_{j=0}^{N-1} e_{i,j}$ for $N \times N$ halftone images representing the input images such that $g_{i,j} = g$ for all $i = 0, 1, \dots, N-1, j = 0, 1, \dots, N-1$. Computations were performed for $N = 16, 32, 48, \dots, 464, g = 1/64, 2/64, \dots, 63/64$. (Zeremba [37] and Shirley [29] developed similar criteria to evaluate quality of non-uniform sampling.) Intensity distortion for an area of a halftone image is the difference between the actual number of white pixels in the area and the number of white pixels needed to preserve the average intensity. The latter may be non-integer. In my study, I chose the sets of possible values g and N so that this was never the case for the whole image. For SACDH, n was set to 192 to avoid rounding. *Intensity distortion per pixel* $d = M/N^2$ was also computed and studied for some of the algorithms. The intensity distortion figures for SACDH turned out to be approximately 6 times lower than those for both void-

and-cluster and an SED algorithm with a special kind of BR designed to remove a distortion component linear in N and $|g - 1/2|$, which was approximately 3 times stronger yet. The intensity distortion caused by rounding is spread over the whole image, hence no extra boundary effects.

Presence of quantization noise decreases contrast sensitivity, and edge enhancement is widely believed to be needed to compensate for that. However, EE is unwanted when a digital halftoning algorithm is applied in digital holography [11]. EE may also cause some of the optical illusions discussed in [14]. Knox [17] showed by measurement that an inherent mechanism for asymmetric EE was built into the classical Floyd–Steinberg ED. In a later paper [18], he provided a partial explanation of the phenomenon and demonstrated that the inherent EE was even stronger in another ED algorithm, yet could not be detected in the halftone images produced using line-by-line *delta-sigma modulation (DSM)*. Sandler et al. [26] provide a few references on DSM. From their results, it follows that, in line-by-line (column-by-column) DSM, the expected values $E(\xi_{i,j})$ remain close to $g_{i,j}$ for all (i, j) for a wide variety of inputs, which explains the latter finding by Knox. Alas, DSM is not a good halftoning algorithm. Extending the approach of Knox [17], I measured EE in halftoned $N \times N$ vertical and horizontal grayscale steps for different halftoning algorithms. Intensity distortion per pixel was computed for the columns of the halftone vertical step images and the lines of the halftone horizontal step images. (Only the steps with the intensity values symmetric with respect to $1/2$ were studied.) The measurement showed that SACDH does not enhance the edges of symmetric grayscale steps. It is straightforward to add relatively isotropic EE to any digital halftoning algorithm. The details can be found in my technical report [15].

4. Conclusions

A new class of digital halftoning algorithms, anti-correlation digital halftoning (ACDH), was introduced. Its representative, serpentine ACDH, causes fewer correlated artifacts and less contouring than the benchmark algorithms. Unlike some of those algorithms, SACDH does not enhance edges or cause significant transient boundary effects.

5. Acknowledgments

The author thanks Paul W. Purdom, Jr., Thomas Zeggel, Jan P. Allebach, Gregory Y. Milman, Robert Ulichney, and Vladimir V. Meňkov for their help and advice. I am deeply grateful to Gregory Pogoyants for his permission to use the digitized portrait of his daughter, Anya Pogoyants (1969–1995). My work was partially supported by NSF Grant CCR 94-02780.

References

1. J. P. Allebach, *Visual Model-Based Algorithms for Halftoning Images*, Proc. of SPIE: Image Quality **310** (1981) pp. 151–157.
2. M. Analoui and J. P. Allebach, *Model Based Halftoning Using Direct Binary Search*, Proc. of SPIE: Human Vision, Visual Processing, and Digital Display III **1666** (1992) pp. 96–108.
3. D. Anastassiou, *Error Diffusion Coding for A/D Conversion*, IEEE Transactions on Circuits and Systems **36** (9) (1989) pp. 1175–1186.
4. B. E. Bayer, *An Optimum Method for Two-Level Rendition of Continuous-Tone Pictures*, Conference Record, IEEE International Conference on Communications **1**, IEEE, New York (1973) pp. (26-11)–(26-15).
5. A. E. Burgess, R. F. Wagner, and R. J. Jennings, *Human Signal Detection Performance for Noisy Medical Images*, Proceedings of the International Workshop on Physics and Engineering in Medical Images, IEEE, New York (1982).
6. F. W. Campbell, J. J. Kulikowski, and J. Z. Levinson, *The Effect of Orientation on the Visual Resolution of Gratings*, Journal of Physiology (London) **187** (1966) pp. 427–436.
7. P. Carnevali, L. Coletti, S. Patarnello, *Image Processing by Simulated Annealing*, IBM Journal of Research and Development **29**(6) (1985) pp. 569–579.
8. P. C. Cosman, R. M. Gray, and R. A. Olshen, *Evaluating Quality of Compressed Medical Images: SNR, Subjective Rating, and Diagnostic Accuracy*, Proc. of the IEEE, **82**(6) (1994) pp. 919–932.
9. R. Eschbach, *Pulse-Density Modulation on Rastered Media: Combining Pulse-Density Modulation and Error Diffusion*, Journal of the Optical Society of America A **7**(4) (1990) pp. 708–716.
10. R. Eschbach and R. Hauck, *Binarization Using a Two-Dimensional Pulse-Density Modulation*, Journal of the Optical Society of America A **4**(10) (1987) pp. 1873–1878.
11. F. Fetthauer and O. Bryngdahl, *Quantization Noise and the Error Diffusion Algorithm*, Journal of Electronic Imaging **3**(1) (1994) pp. 37–44.
12. R. W. Floyd and L. Steinberg, *An Adaptive Algorithm for Spatial Grey Scale*, SID 75 Digest, Society for Information Display (1975) pp. 36–37.
13. R. W. Floyd and L. Steinberg, *An Adaptive Algorithm for Spatial Greyscale*, Proc. of Society for Information Display **17**(2) (1976) pp. 75–77.
14. S. Grossberg and D. Todorović, *Neural Dynamics of 1-D and 2-D Brightness Perception: A Unified Model of Classical and Recent Phenomena*, in: S. Grossberg (Ed.), *Neural Networks and Natural Intelligence*, The MIT Press, Cambridge, Mass. (1988) pp. 127–194.
15. D. A. Gusev, *Anti-Correlation Digital Halftoning*, TR No. 513, Computer Science Department, Indiana University, Bloomington (1998) 87 pages, <ftp://ftp.cs.indiana.edu/pub/techreports/TR513.ps.Z>
16. D. A. Gusev, G. Y. Milman, E. A. Sandler, *Principles of Optimal Rasters Application to Pattern Recognition Problems*, in: N. N. Evtukhiev (Ed.), *Voprosy Kibernetiki, Ustroystva i Sistemy* (MIREA Transactions), Moscow Institute of Radioengineering, Electronics, and Automation, Moscow (1992) pp. 18–29 [in Russian].
17. K. T. Knox, *Edge Enhancement in Error Diffusion*, Advance Printing of Paper Summaries: SPSE's 42nd Annual Conference (1989) pp. 310–313.
18. K. T. Knox, *Error Image in Error Diffusion*, Proc. of SPIE: Image Processing Algorithms and Techniques III **1657** (1992) pp. 268–279.
19. D. E. Knuth, *Digital Halftones by Dot Diffusion*, ACM Transactions on Graphics **6**(4) (1987) pp. 245–273.
20. M. Y. Lermontov, *Hero of Our Time*, Otechestvennye Zapiski, Saint Petersburg (1839).
21. P. Li, J. P. Allebach, *Look-Up-Table Based Halftoning Algorithm*, Proc. of ICIP-98: 1998 IEEE International Conference on Image Processing VI (1998).
22. T. Mitsa and K. J. Parker, *Digital Halftoning Technique Using a Blue-Noise Mask*, Journal of the Optical Society of America A **9**(11) (1992) pp. 1920–1929.
23. K. J. Myers, H. H. Barrett, M. C. Borgstrom, D. D. Patton, and G. W. Seeley, *Effect of Noise Correlation on Detectability of Disk Signals in Medical Imaging*, Journal of the Optical Society of America A **2** (1985) pp. 1752–1759.
24. D. F. Rogers, *Procedural Elements for Computer Graphics*, McGraw-Hill, New York (1985).
25. E. A. Sandler, D. A. Gusev, and G. Y. Milman, *Hybrid Algorithms for Digital Halftoning and Their Application to Medical Imaging*, Computers & Graphics **21**(1,6) (1997) pp. 69–78, 859 (erratum).
26. E. A. Sandler, D. A. Gusev, G. Y. Milman, M. L. Podolsky, *Estimating from Outputs of Oversampled Delta-Sigma Modulation*, Signal Processing **59**(3) (1997) pp. 305–311.
27. T. Scheermesser and O. Bryngdahl, *Texture Metric of Halftoning Images*, Journal of the Optical Society of America A **13**(1) (1996) pp. 18–24.
28. M. A. Seldowitz, J. P. Allebach, and D. W. Sweeney, *Synthesis of Digital Holograms by Direct Binary Search*, Applied Optics **26**(14) (1987) pp. 2788–2798.
29. P. Shirley, *Discrepancy as a Quality Measure for Sample Distributions*, in: F. H. Post and W. Barth (Eds.), *Proc. of Eurographics '91*, North Holland, Amsterdam (1991) pp. 183–194.
30. R. L. Stevenson and G. R. Arce, *Binary Display of Hexagonally Sampled Continuous-Tone Images*, Journal of the Optical Society of America A **2** (1985) pp. 1009–1013.
31. R. Ulichney, *Digital Halftoning*, The MIT Press, Cambridge, Mass. (1987).
32. R. Ulichney, *Frequency Analysis of Ordered Dither*, Proc. of SPIE: Hard Copy Output **1079** (1989) pp. 361–373.
33. R. Ulichney, *The Void-and-Cluster Method for Dither Array Generation*, Proc. of SPIE: Human Vision, Visual Processing, and Digital Display IV **1913** (1993) pp. 332–343.
34. T. Zeggel, O. Bryngdahl, *Halftoning with Error Diffusion on an Image-Adaptive Raster*, Journal of Electronic Imaging **3**(3) (1994) pp. 288–294.
35. T. Zeggel, O. Bryngdahl, *Halftoning with Iterative Convolution Algorithm*, Optics Communications **118**(5,6) (1995) pp. 484–490.
36. T. Zeggel, O. Bryngdahl, *Gradient-Controlled Iterative Half-Toning*, Applied Optics **36**(2) (1997) pp. 423–429.
37. S. K. Zeremba, *The Mathematical Basis of Monte Carlo and Quasi-Monte Carlo Methods*, SIAM Review **10**(3) (1968) pp. 303–314.



Figure 1: Portrait of Anya Pogoyants, 300 dpi.
 a) Ordered dither with a recursive tessellation matrix.
 b) Ordered dither with a blue noise mask (void-and-cluster).
 c) Three-weight serpentine error diffusion.
 d) Error diffusion combined with pulse-density modulation.
 e) The iterative convolution algorithm.
 f) Serpentine anti-correlation digital halftoning.

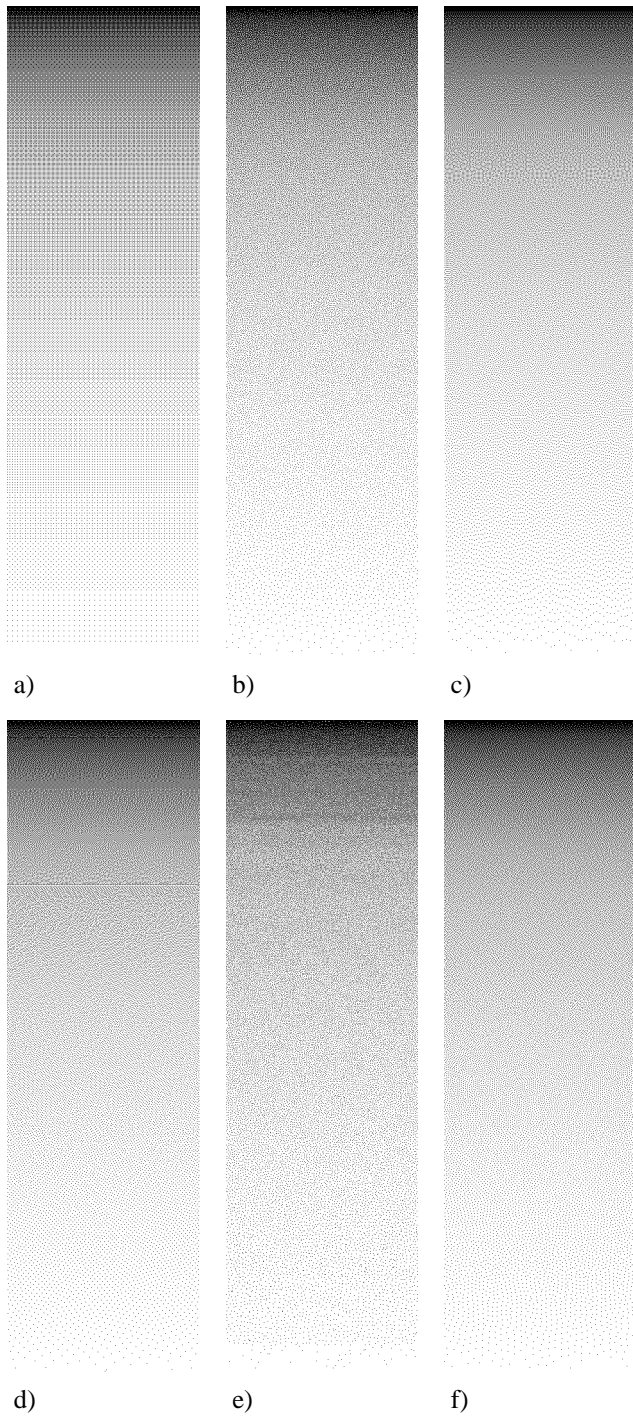


Figure 2: Gray scale ramp, 300 dpi.
 a) Ordered dither with a recursive tessellation matrix.
 b) Ordered dither with a blue noise mask (void-and-cluster).
 c) Three-weight serpentine error diffusion.
 d) Error diffusion combined with pulse-density modulation.
 e) The iterative convolution algorithm.
 f) Serpentine anti-correlation digital halftoning.